World Journal of Advanced Research and Reviews
eISSN: 2581-9615 CODEN (USA): WJARAI
Cross Ref DOI: 10.30574/wjarr
Journal homepage: https://wjarr.com/

(RESEARCH ARTICLE)

Check for updates

Basement depth re-valuation of anomalous magnetic bodies in the lower and middle Benue trough using Euler deconvolution and spectral inversion techniques

Ibe Alexander Omenikolo [1,*], Terhemba Theophilus Emberga [1] and Alexander Iheanyichukwu Opara [2]

[1] *Department of Physics/Electronics, Federal Polytechnic Nekede, P; M; B; 1036, Owerri, Nigeria.*
[2] *Department of Geology, Federal University of Technology, P; M; B; 1526 Owerri, Nigeria.*

World Journal of Advanced Research and Reviews, 2022, 14(02), 129–145

Publication history: Received on 21 March 2022; revised on 04 May 2022; accepted on 06 May 2022

Article DOI: https://doi.org/10.30574/wjarr.2022.14.2.0356

Abstract

Spectral technique and Euler Deconvolution were applied to high-resolution aeromagnetic data of parts of Benue trough to estimate the depth of anomalous magnetic sources within the study area; Data enhancement techniques such as total magnetic intensity map, reduction to pole, regional-residual separation and upward continuation maps were employed to identify different magnetic anomalies, structural trends representing the tectonics of the location were observed trending NE-SW and N-S directions; The result of 3D Euler deconvolution for the structural index (SI) = 0, 1, 2, 3 gave depths to magnetic sources that range from -589;3 m to -2678;8 m, -459;0 m to -2691;9 m, -294;6 m to -2817;5 m, -430;2 m to -2780;6 m respectively; The depth estimates from 2-D spectral revealed a two-layer model; The shallow magnetic depth ranges between 0;135 km to 0;200 km with a mean depth of 0;158 km and the depth to magnetic basement vary between 2;585 km to 4;878 km with a mean depth of 3;415 km; This result, therefore, indicates that the average basement depth of the study area obtained from the spectral analysis is 3;415km; This investigation, therefore provides appropriate sedimentary thickness for suitable hydrocarbon prospecting within the study area.

Keywords: Basement depth; Spectral analysis; Upward continuation; Reduction to pole; Magnetic anomalies.

1. Introduction

The magnetic survey is one of the most reliable tools used in geophysical surveys for the investigation of surface and subsurface geology. The magnetic method measures variations in the Earth's magnetic field as a result of the anomalies in the geomagnetic field which are the resultant effects of the magnetic properties of the underlying rocks. It is applied for exploring hydrocarbon, minerals and for archaeological studies. In prospecting for oil, estimating depth to magnetic source bodies, possibly sediment thickness and in delineating subsurface structures. It is suitable for locating buried magnetic ore bodies due to their magnetic susceptibilities [16].

The aeromagnetic method has exhibited a remarkable role as regards quick coverage, rapid speed, reduced cost and having access to inaccessible terrains [4,7,40]. The technique has also been noted as a principal mapping tool for materials that are strongly magnetized [18]. Magnetic data are very effective in indicating the presence, delineating the boundaries, and determining the depth of igneous rocks [9,35,36]. Estimation of relief on the basement surface may be related to structures that harbour hydrocarbon in overlying sedimentary basins [8]. Several studies have been carried out for the estimation of depth to the basement using the spectral inversion method and 3D Euler Deconvolution [8,13,15,23-24,30-32,44,47,49,50]. Ofoegbu [51] estimated the thickness of the sediments in the Lower and Middle Benue Trough to vary between 0.5 and 7.0 km. Ekwok et al. [8] evaluated the depth to magnetic sources in parts of Southeastern Nigeria, standard Euler deconvolution, source parameter imaging, spectral depth analysis and two dimensions (2-D) forward modelling was applied to the airborne magnetic data. The results from the techniques

* Corresponding author: Omenikolo IA
Department of Physics/Electronics, Federal Polytechnic Nekede, P.M.B. 1036, Owerri, Nigeria.

correlated strongly with each other in the study area. In the study carried out by Umeanoh et al. [50] For 3D Euler, using structural index (SI) = 1 the depth varies between 1525.74 km to 2919.21 km, for SI = 2 and 3, the depth varies between 2290.49 km to 4447.62 km and 925. 93 km to 5790.49 km respectively. Obiora et al. [23] using Standard Euler deconvolution for the structural index (SI) of 0.5, 1.0, 2.0 and 3.0, observed depths to magnetic sources ranging from 0 to 1500 m, 300 to 3300 m, 0 to 4000 m and 200 to 4200 m, respectively.

2. Location and Geology of the Study Area

The study area is located within the Benue Trough, Nigeria within latitudes 5° 00¹N - 8° 00¹N and Longitude 7° 00¹ E - 9° 30¹E. Figure 1 is the location of the study area.

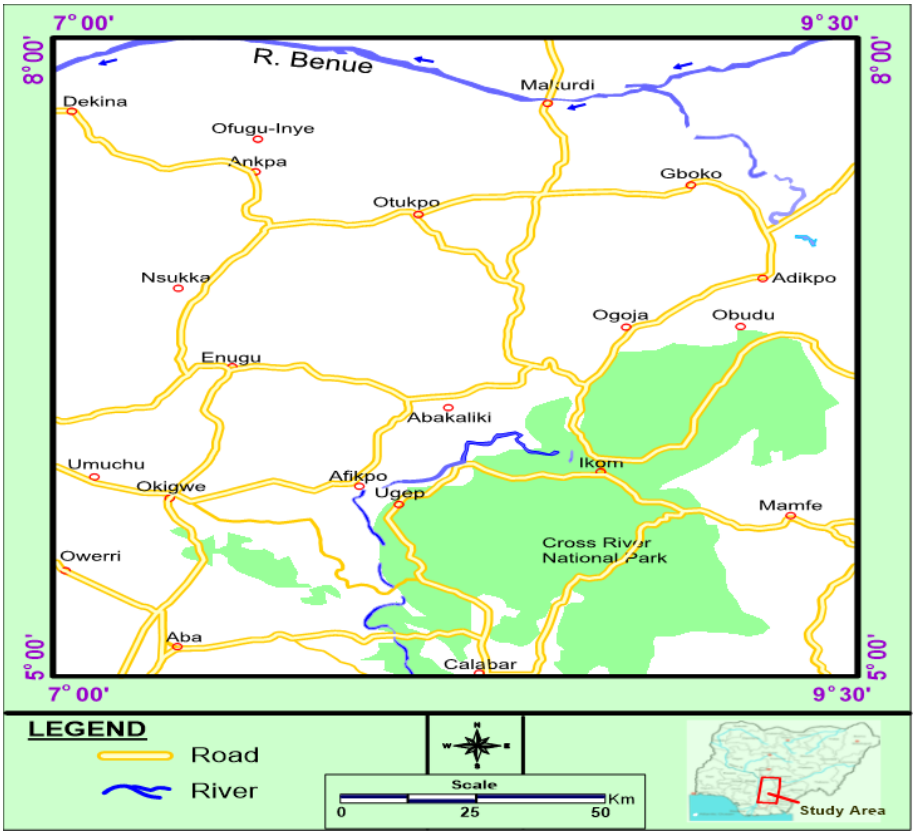

Figure 1 Location map of the study area

The Benue trough is a Cretaceous folded rift basin that lies across Nigeria. It has an extension from the Niger Delta through the Gongola Rift to the Chad Basin in the north. It is a NE-SW trending sedimentary basin, subdivided into the lower, middle and upper Benue troughs. It extends for about 1000 km in length (NE-SW direction) with widths ranging from 180 km to 250 km (Whiteman, [45]). The Benue Trough is part of the long stretch arm of the Central African rift system originating from the early Cretaceous rifting of the Central West African basement uplift [21]. Figure 2 is the geologic map showing the study area. The tectonic evolution of the Benue Trough originated from the separation of the African continent from the South American continent in the Aptian [10]. The study area is characterized by the presence of a thick sedimentary cover of varied composition whose age ranges from Albian to Maastrichtian, with the earliest being the marine Asu-River group of Albian age [21]. Asu-River Group is the oldest sedimentary section deposited on the basement in the Benue Trough [6]. It consists of shales, limestones, sandstones and siltstones. This was followed by Ezeaku Formation during the Turonian regression period and comprised of argillite, with occasional beds of limestone, carbonate and shale. Others include Keana/Awe Formation, Awgu Formation and Lafia sandstone as the youngest sediment [21].

The event of the stages of deposition in Benue trough is distinguished by periods of marine regression and transgression [17,39,42]. Series of tectonic activities affected the sedimentary sequences in the trough, resulting in two stages, the Cenomanian and the Santonian deformations [19,26]. The Santonian was distinguished by series of compressive folding, trending along NE-SW direction and parallel to the Trough margin. The emergence of Abakaliki Anticlinorium was

affected as a result of the folding episode which occurred during the Santonian deformation. The compressional nature of the folds that significantly evolved during this era is shown by their asymmetry and the reversed faults associated with them. Benkhelil [3] in a study on the geology of Abakaliki, suggested that the compression responsible for the large-scale folding and cleavage was directed N155 ° E. The magmatism that took place gave rise to the injection of numerous intrusive bodies into the shale of the Eze Aku and Asu River Group. The Cenomanian deformation affected only Albian sediments. The lithostratigraphy of the Benue trough comprises formations ranging from Cretaceous to tertiary in age.

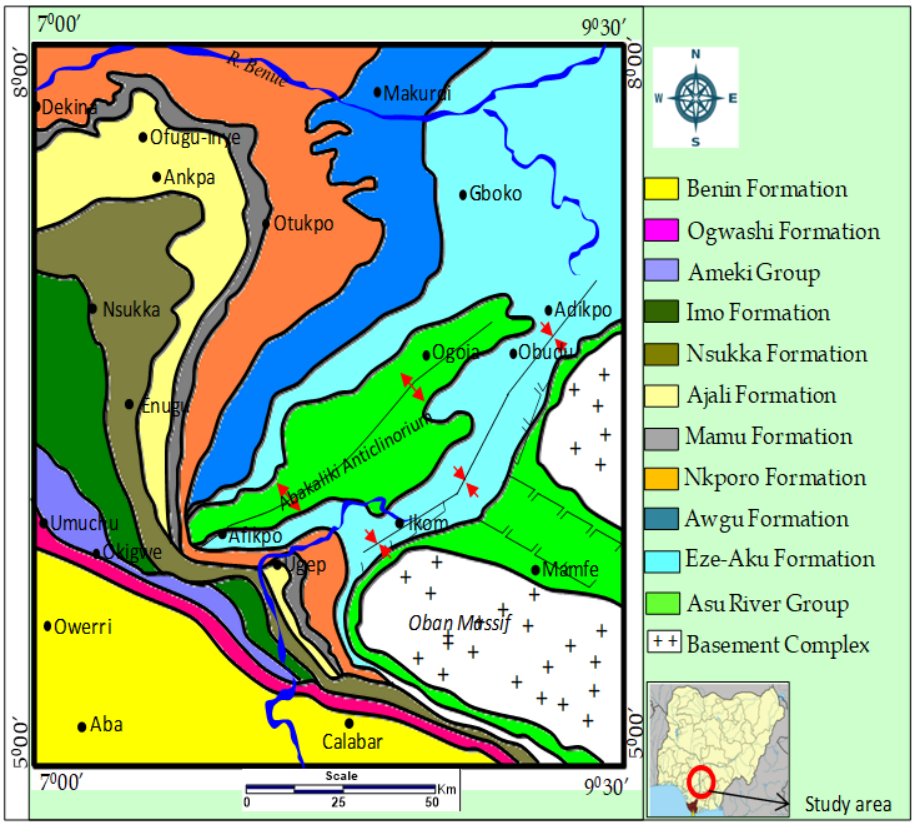

Figure 2 Geologic map of the study area showing the structural elements [21]

3. Material and methods

Twenty-nine (29) aeromagnetic datasets used for this study are, part of the new high resolution digital airborne data acquired and preliminary processed between 2005 and 2009. The maps were digitized along flight lines with a spacing of 500m and 80m terrain clearance, the intersection points were picked and contoured using the Oasis Montaj Software. Fugro Airborne Surveys carried out the data acquisition while the processing and preliminary interpretations were handled by Paterson, Grant & Watson Limited (PGW). The nationwide grid subset covering the research area (latitude 5° 00¹N to 8° 00¹N and longitude 7° 00¹ E to 9° 30¹E) was provided in Geosoft .xyz format. The tie-lines and flight lines orientation were in NE-SW and NW-SE direction respectively. The International Geomagnetic Reference Field (IGRF) formula for 2005 was used to remove the geomagnetic gradient from the data processing of the aeromagnetic data was done using the Oasis Montaj, Surfer 13, and potent software package. Production of the total magnetic intensity (TMI) grid of the study area using Oasis Montaj software was done by merging the twenty-nine (29) aeromagnetic datasheets. The aeromagnetic sheet was merged and divided into 32 overlapping sections. Each of these sections covers a square area of about 27.5km x 27.5km of the datasheet, to accommodate longer wavelengths so that deeper depths could be investigated. Removal of regional anomalies from the total magnetic intensity was carried out to obtain the residual anomaly using polynomial fittings. The different data enhancement techniques applied include a reduction to the equator and upward Continuation.

3.1. Reduction to the Pole (RTP)

Reduction to the Pole (RTP) transformation corrects for the offset between the locations of anomalies (closed highs or lows on a contour map) and their sources which is a consequence of the vector nature of the Earth's magnetic field. The

application of Reduction to Pole (RTP) transformation on aeromagnetic data ensures the minimization of polarity effects [4].

To apply the reduced-to-pole transformation correctly, one must assume that the total magnetizations of most rocks in the study area align parallel or anti-parallel to the Earth's main field. This approach makes it possible to determine from the observed total field the position and depth of the pole that has the magnetic effect equivalent to that of an external source with the inclined magnetization. This technique transforms induced magnetic responses to those that would arise where the sources are placed at the magnetic pole (vertical field). This simplifies the interpretation because, for sub-vertical prisms or sub-vertical contacts (including faults), it transforms their asymmetric responses to simpler symmetric and anti-symmetric forms. The symmetric 'highs' are directly centered on the body, while the maximum gradient of the anti-symmetric dipolar anomalies coincides exactly with the body edge. Pole reduction is difficult at low magnetic latitudes since N-S bodies have no detectable induced magnetic anomaly at zero geomagnetic inclination. Pole reduction is not a valid technique where there are appreciable remanence effects.

3.2. Upward continuation

This involves the estimation of the potential field at an elevation higher than that at which the field is measured and is applied in assessing the regional magnetic and gravity data. This method provides one to assess the effect of deeper sources because the effect of shallower, short-wavelength features is attenuated. A potential field measured on a given observation plane at a constant height can be reevaluated as though the observations were made on a different plane, either at higher or lower elevations. As described by [11], the process has a frequency response of $e^{-h}(u^2 + v^2)^{½}$ (here h, is the elevation).

For upward continuation, where z is positive downward [43].

$$\mathrm{F}(x, \mathrm{y}, -\mathrm{h}) = \frac{\mathrm{h}}{2\pi} \int\int \frac{F(x,y,o)\partial x \partial y}{\{(x-x')+(y+y')+h^2\}^{1/2}} \quad (1)$$

$F(x, y. -h)$ = Total field at the point P $(x', y', -h)$ above the surface of which $F(x, y. 0)$ is known. h = elevation above the surface.

3.3. Spectral analysis

Spectral analysis is employed for estimating and interpreting magnetic data. This involves estimates of the magnetic basement and shallow depths. This technique is now well established [5,12,52]. The technique involves applying Fourier transform to digitized aeromagnetic data to estimate the energy/amplitude spectrum which is plotted on a logarithmic scale against frequency. This shows a line segment that decreases in slope with an increase in frequency. This decrease in slope shows the depth of the magnetic sources [24]. Given a residual magnetic anomaly map of dimension L×L digitized at equal intervals, the residual intervals, and total intensity anomaly values can be expressed in terms of double Fourier series expansion which is given by:

$$T(x, y) = \sum_{n=1}^{N} \sum_{m=1}^{M} P_m^n cos\left(\frac{2\pi}{L}\right)(nx + my) + Q_m^n sin\left[\left(\frac{2\pi}{L}\right)(nx + my)\right] \quad (2)$$

Where:

L = dimension of the block

$P^n{}_m$ and $Q^n{}_m$ = Fourier amplitude and

N, M = the number of grid points along with the x and y directions respectively.

Combining equation (2) into a single partial wave, we have:

$$P_m^n cos\left[\left(\frac{2\pi}{L}\right)(nx + my)\right] + Q_m^n sin\left[\left(\frac{2\pi}{L}\right)(nx + my)\right] = C_m^n cos\left[\left(\frac{2\pi}{L}\right)(nx + my)\right] - \delta_m^n \quad (3)$$

Where $(P_m^n)^2 + (Q_m^n)^2 = (C_m^n)^2$ (4)

and δ_m^n is the appropriate phase angle.

Each (C_m^n) is the amplitude of the partial wave. The frequency of this wave is given by: $F_m^n = \sqrt{n^2 + m^2}$ is called the frequency of the wave. Similarly, using the complex form, the two-dimensional Fourier transform pair may be written [5].

$$G(U,V) = \int_{-\infty}^{\infty} g(x,y)e^{-j(ux+vy)}dxdy \quad (5)$$

$$g(x,y) = \frac{1}{4\pi^2}\int_{-\infty}^{\infty}\int_{-\infty}^{\infty} G(U,V)e^{-j(ux+vy)}dxdy \quad (6)$$

Where u and v are the angular frequencies in the x and y directions respectively. Some inherent problems in the application of the Discrete Fourier Transform (DFT) include; aliasing, truncation effect or Gibb's phenomenon and the problem associated with even and odd symmetries of the real and imaginary part of the Fourier transform. Kearey et al. [16], stated that aliasing can be overcome by having the sampling frequency of the digitized magnetic field interval be at least twice as high as the highest frequency component present in the sampled function. By applying a cosine taper to the observed data before Fourier Transform, truncation effect can be reduced. In this study, the software used in the analysis took into consideration these effects.

3.4. 3-D Euler Deconvolution

The 3-D Euler deconvolution technique provides the possibility of estimating the depth as well as locations of anomalous magnetic bodies. It also provides information about the geometry of the magnetic bodies. The Euler homogeneity equation relates the magnetic field and its gradient components to the source location with the degree of homogeneity N, which can be represented as a structural index [53]. The technique uses structural index in addition to producing depth estimates. This combined approach has the ability to identify and perform depth estimates for a variety of geologic structures such as dykes, faults, sphere, contact, cylinder with each target characterized by a specific structural index (SI). For example, N = 0 for geologic contact, N = 1 for thin dyke or sill, N = 2 for horizontal or vertical cylinder, and N = 3 for magnetic sphere or dipole [38].

The 3-D Euler deconvolution is based on solving Euler's homogeneity equation [53].

$$(x - x_0)\frac{\partial F}{\partial x} + (y - y_0)\frac{\partial F}{\partial y} + (z - z_0)\frac{\partial F}{\partial z} = N(B - F) \quad (7)$$

where the derivatives of the field are $\frac{\partial F}{\partial x}, \frac{\partial F}{\partial y}, \frac{\partial F}{\partial z}$ in the x, y, and z directions respectively, the structural index is given as N, while the regional value of the total magnetic field is B, and (x_0, y_0, z_0) is the magnetic source position which generates the total magnetic field F measured at (x, y, z).

Table 1 Structural indices for simple magnetic models used for depth estimate by 3-D Euler deconvolution (adapted after [37])

Geologic Model	Number of Infinite Dimensions	Magnetic Structural Index
Sphere	0	3
Pipe	1(x)	2
Horizontal Cylinder	1(x-y)	2
Dyke	2(x and x-y)	1
Sill	2(x and y)	1
Contact	3(x,y,z)	0

4. Results and discussion

Figure 3 is the Total Magnetic Intensity Map (TMI) of the study area produced using Oasis Montaj software. The TMI map reveals magnetic intensity values ranging from -94.2 nT to 142.6 nT. The map indicates two distinct magnetic structural trends of high and low relief. The colour legend bar shows areas having high (pink colour) and low (blue

colour) magnetic signatures. The high relief area is therefore more tectonically active than the low relief area owing to the presence of many intrusive bodies present in the area. Also, this variation could be attributed to several factors such as, the difference in susceptibility, variation in-depth, degree of strike and difference in lithology. The circular contours are areas of basic intrusives with ore bodies. Magnetic highs were observed around Ankpa, Oturkpo, and Markudi while Magnetic lows are observed around Ejekwa, Ogoja, Gboko, and Katsina-ala areas.

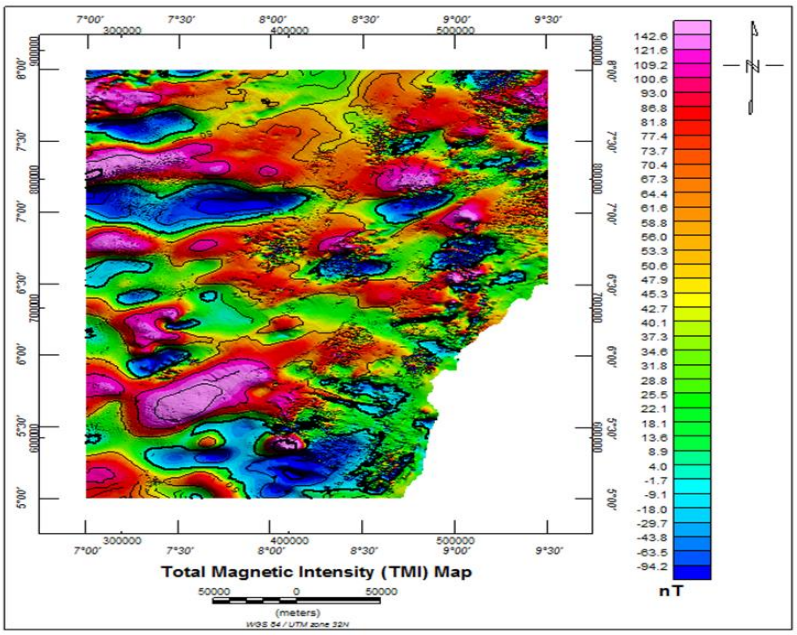

Figure 3 Total Magnetic Intensity (TMI) Image of the study area

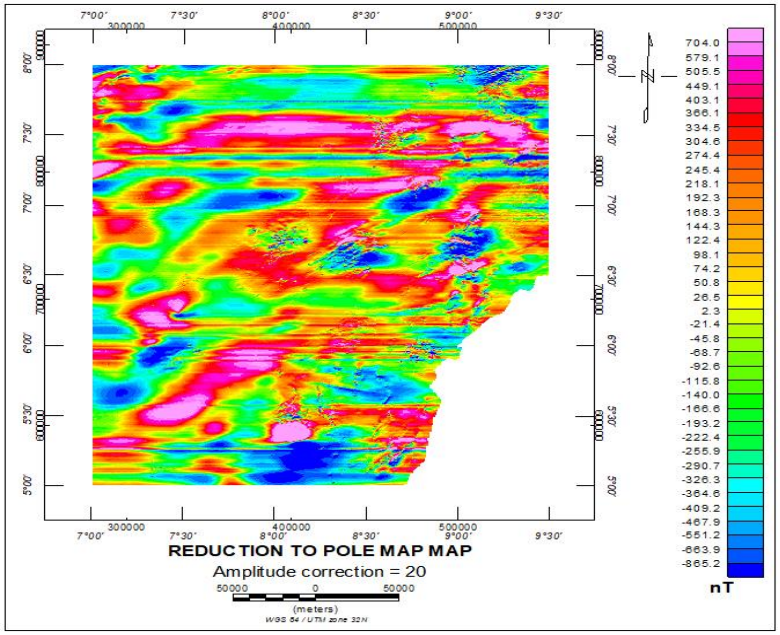

Figure 4 Reduction to pole Map of the Study Area

Figure 4 is the reduction to pole map, it reflects the shift in the positions of the magnetic anomalies and the shapes centered over their respective causative sources. The RTP map reveals high and low magnetic anomalies with different patterns within the study area. The RTP anomaly map ranges between -865.2 nT and 704.0 nT. The colour-shaded RTP map reveals high magnetic responses depicted by purple colour on the legend, it ranging from 505.5 nT to 704.0 nT which dominated the northeastern and southern part of the study. These anomalies are trending NE-SW and N-S. The

medium is depicted by yellow to a green colour ranging from -290.7 nT to 28.5 nT and seen basically in the central and northern part of the study area. Towards the Southern and Northeastern part of the RTP map, the area is characterized by a relatively low magnetic intensity `value from -467.2 nT to -865.2 nT marked with blue colour. The closed contours represent high magnetic signatures linked to shallow structures such as contacts, fractures and intrusive bodies [41]. Reynold et al. [40] and Opara [31] have associated the series of low magnetic closures with linear trends, which initiate shear/fault zones.

The first degree regional and residual magnetic maps generated from the total magnetic intensity map using the polynomial fitting technique are shown in Figures 5 and 6. Multi-regression least-squares analysis was used to remove regional gradient by fitting a plane surface to the data. From the first degree on the residual map of the study area, very low residual magnetic intensity occurs towards the Southern and Southeastern parts of the map, depicted in blue colours. However, very low residual magnetic intensity ranges between -88.8nT to -35 nT. These areas coincide with the underlying Asu River Group, Eze Aku Group, and Biotite Granite and are therefore classified as areas with magnetic low. These areas of low residual magnetic intensities can be qualitatively interpreted as zones of low magnetization, which implies the non-existence of underlying shallow to near-surface magnetized bodies. The major magnetic highs in the study are observed around areas that coincide with the underlying Nkporo Group, Eze Aku Group. These areas are depicted with purple colouration and have residual magnetic intensity values between 53.1nT to 72.8nT. These areas of high residual magnetic intensities can therefore be qualitatively interpreted as zones of high magnetization, which implies the existence of underlying shallow to near-surface magnetized bodies.

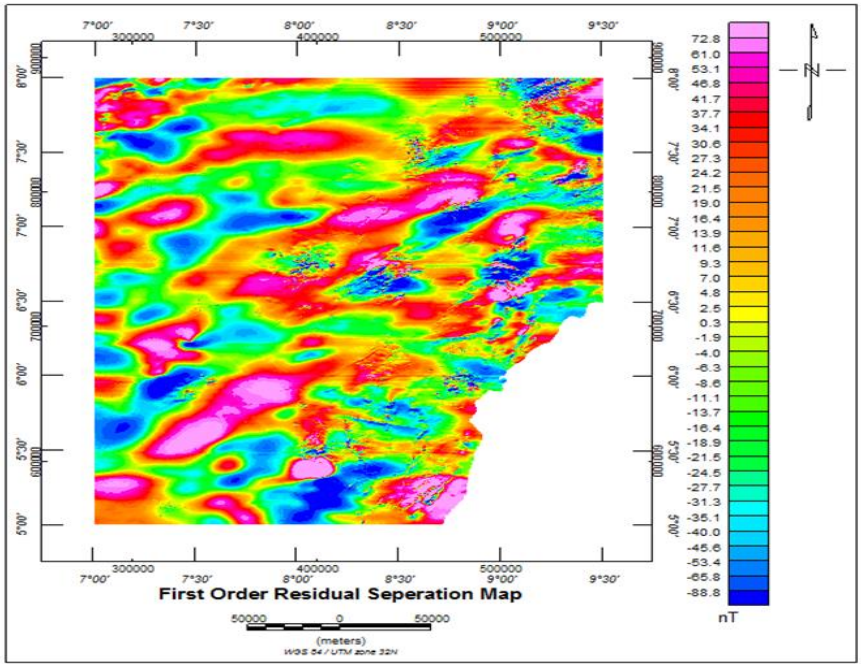

Figure 5 First Residual magnetic intensity map of the study area

First-degree regional anomalies of the aeromagnetic data reveal a dominant regional trend NE-SW trends with values ranging from -52.4nT to 118.1nT. This result is in agreement with previous studies which suggested that Nigeria has a complex network of fractures and lineaments with dominant trends of NW-SE, NE-SW, N-S, and E-W directions [2,6].

Upward continuation is applied to magnetic data to estimate the regional anomaly over an area since the regional field is presumed to exist from deep sources. It is relevant in interpreting magnetic fields containing shallow magnetic features like dykes and other intrusive [16]. It enhances the anomalies of the deep-seated structures and suppresses the effect of shallow anomalies. Figures 7, 8 and 9 show the RTP upward continued to 1000 m, 2000 m and 4000 m. The upward continuation map becomes sharper and smoother at various levels with increasing height. This is a result of the attenuation of the short-wavelength anomalies from shallow features to enable easy interpretation of deep sources. As the continuation distance is increased, the effects of smaller, narrower and thinner magnetic bodies progressively disappear relative to the effects of larger magnetic bodies of considerable depth extent. Upward continuation maps provide evidence of the main tectonic and crustal blocks in an area. For 4000m (Figure 9), the regional fields reveal a better sharp and smooth images trending in SW-NE direction as seen on the TMI, residual and regional maps

respectively. The areas having purple colour on the legend indicate areas of high magnetic intensity while areas with blue colour show areas of low magnetic intensity as indicated by the colour legend bar.

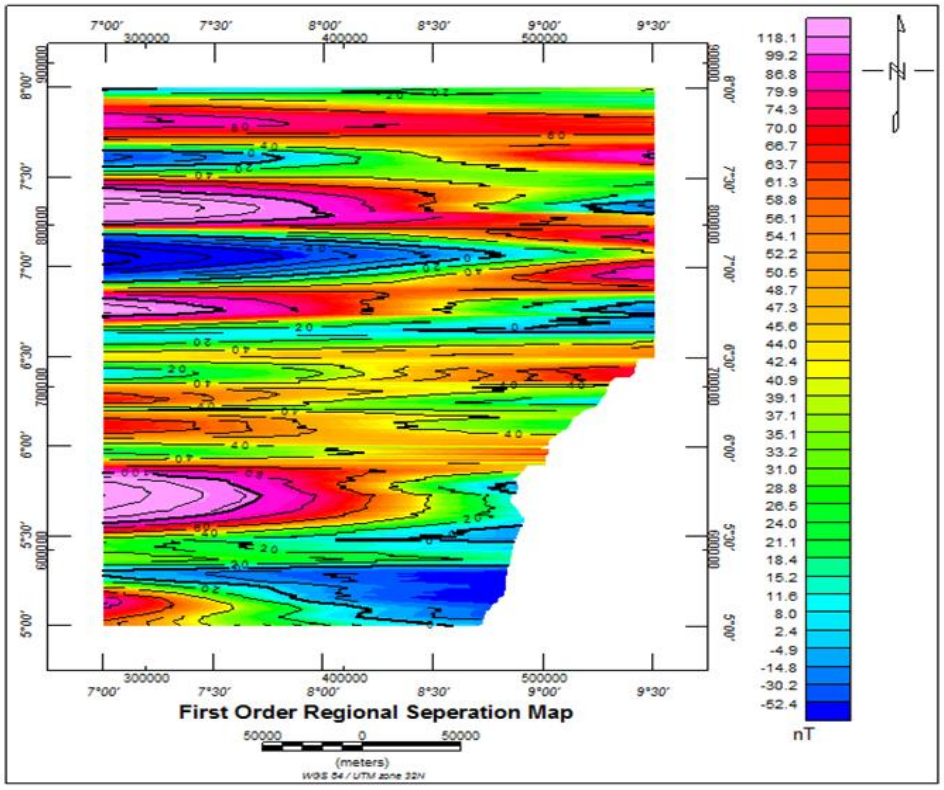

Figure 6 First Degree Regional Field over the Study Area as a contour map

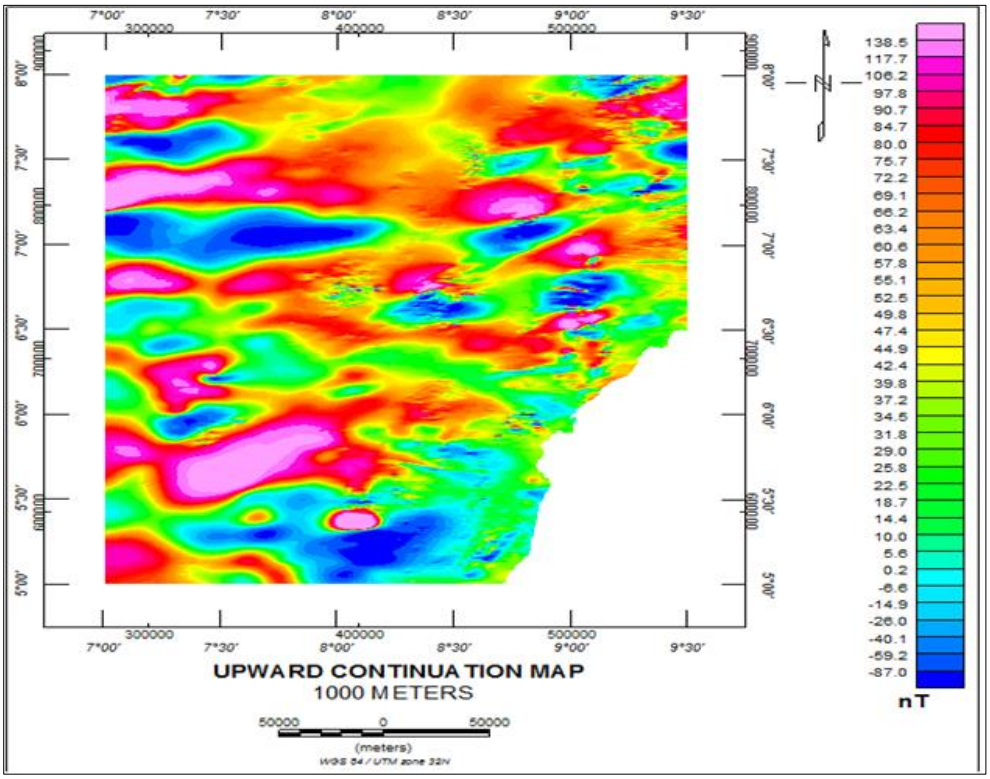

Figure 7 Upward continuation at 1000 m

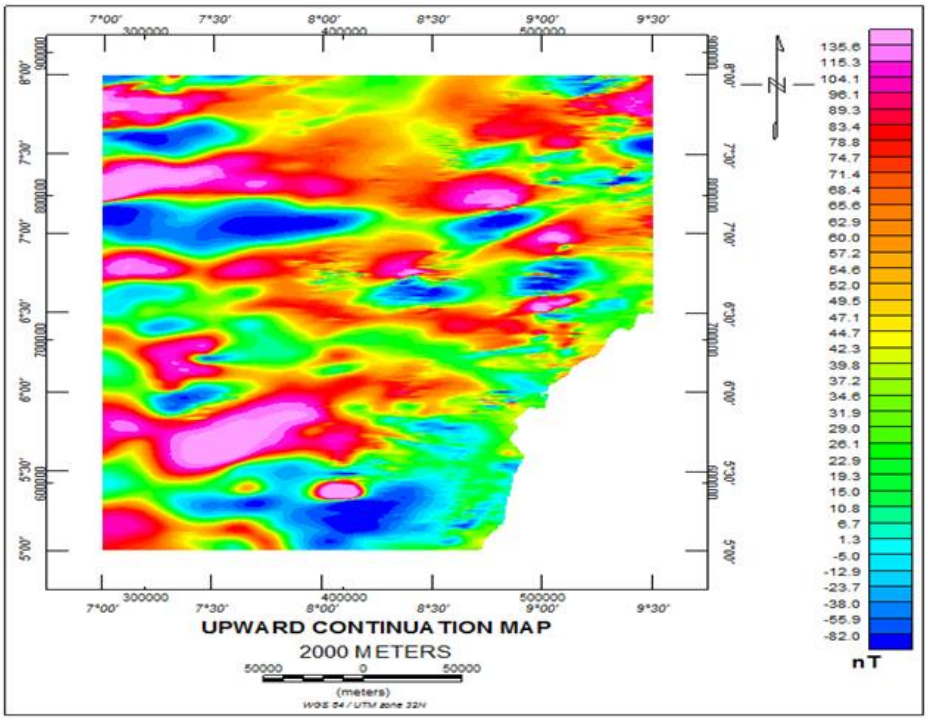

Figure 8 Upward continuation at 2000 m

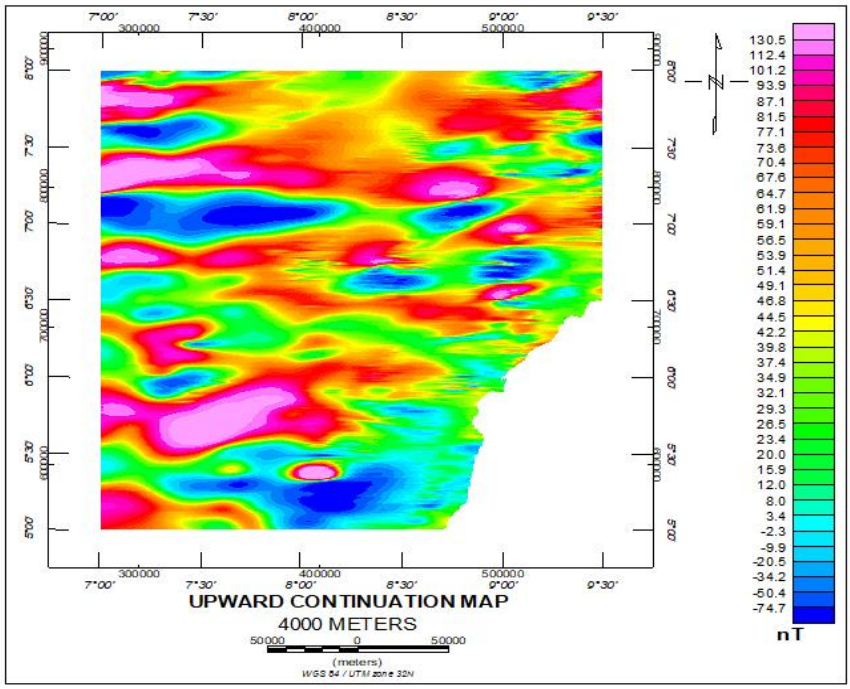

Figure 9 Upward continuation at 4000 m

3D Euler deconvolution was carried out by employing Oasis Montaj software to estimate the Euler depth and to produce the Euler depth map. Four 3D Euler maps were generated for four different structural index Euler depth SI = 0, 1, 2, 3 as shown in Figures 10, 11, 12, and 13. From the Euler maps, the blue colour indicates deep-lying magnetic bodies, while the pink colour on the legend signifies areas of shallow magnetic bodies which in many cases are characterized by low sediment thickness. Figures 10, 11, 12&13 show the result obtained for the structural index of 0 (contacts) with depths ranging from -589.3 m to -2678.8m, SI = 1 (sills and dykes) varies between -459.0 m to -2691.9 m, for SI=2 (horizontal

cylinders and pipes) depth ranges from -294.6 m to -2817.5 m, SI=3 (spheres) depth ranges from - 430.2 m to -2780.6 m and a concentration of clustered solutions in the northeastern and southeastern part of the study area. The result of the 3D Euler depths estimation is summarized in Table 2.

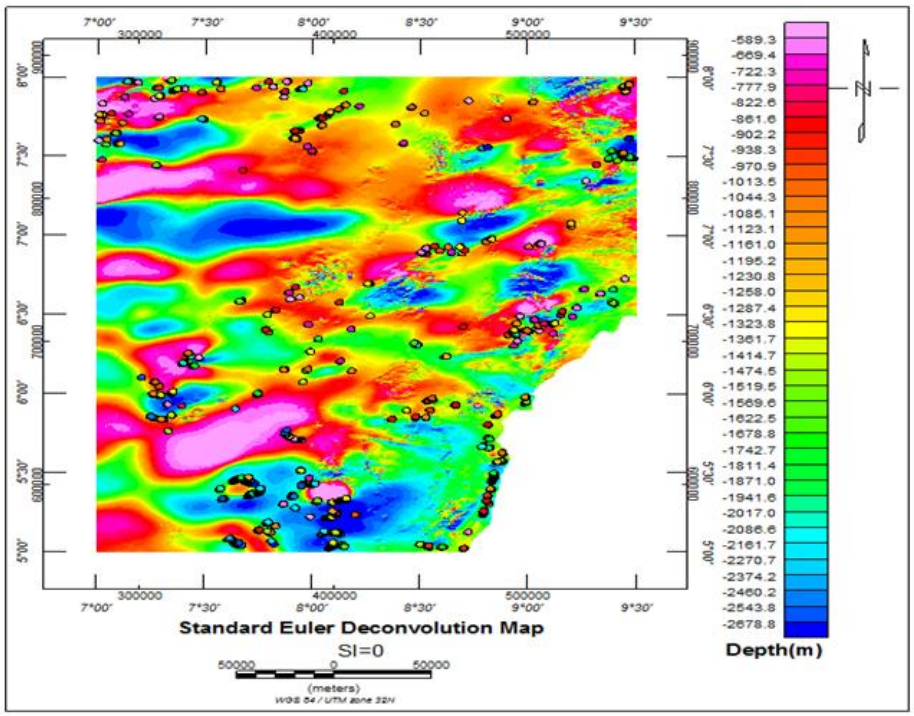

Figure 10 3D Euler deconvolution for SI = 0

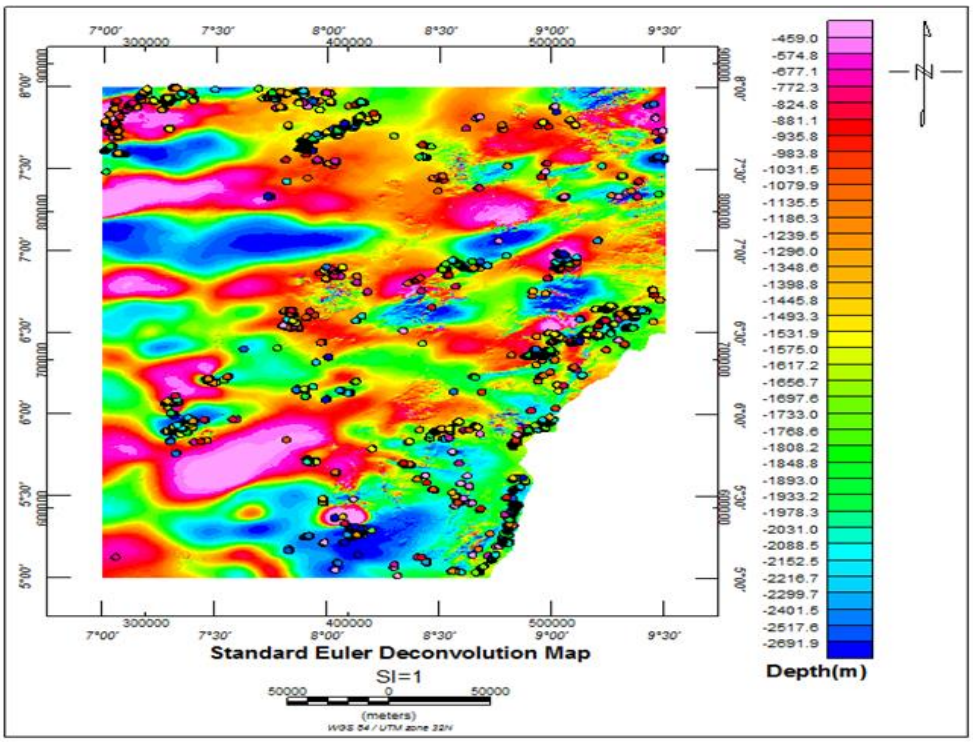

Figure 11 3D Euler deconvolution for SI = 1

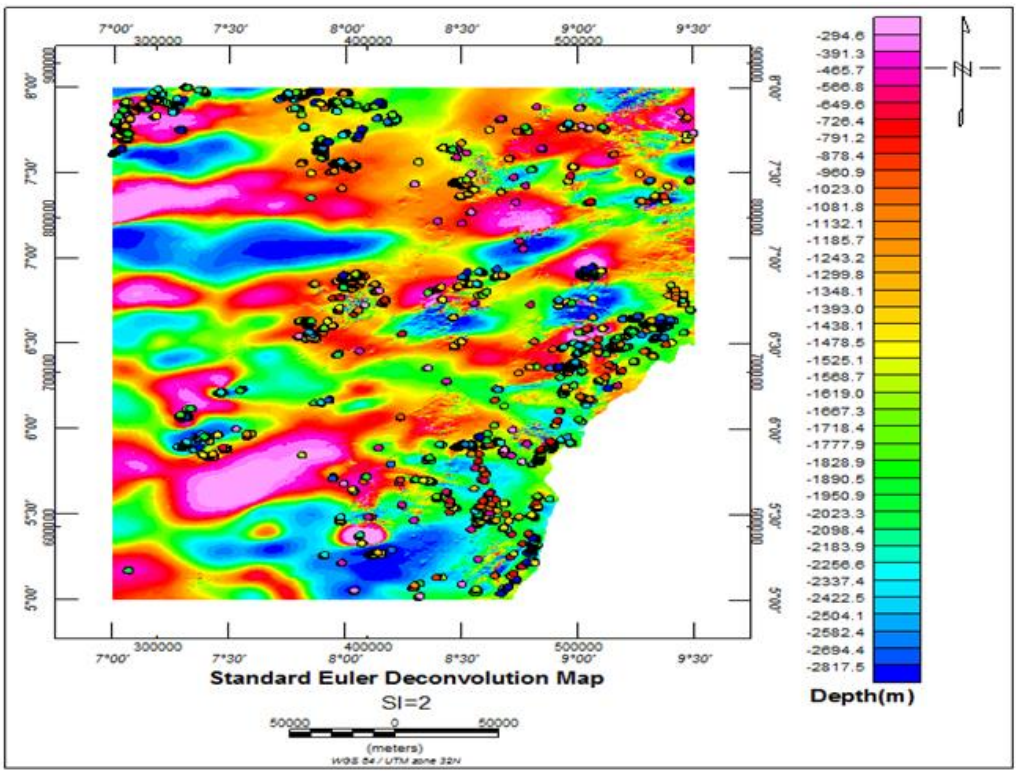

Figure 12 3D Euler deconvolution for SI = 2

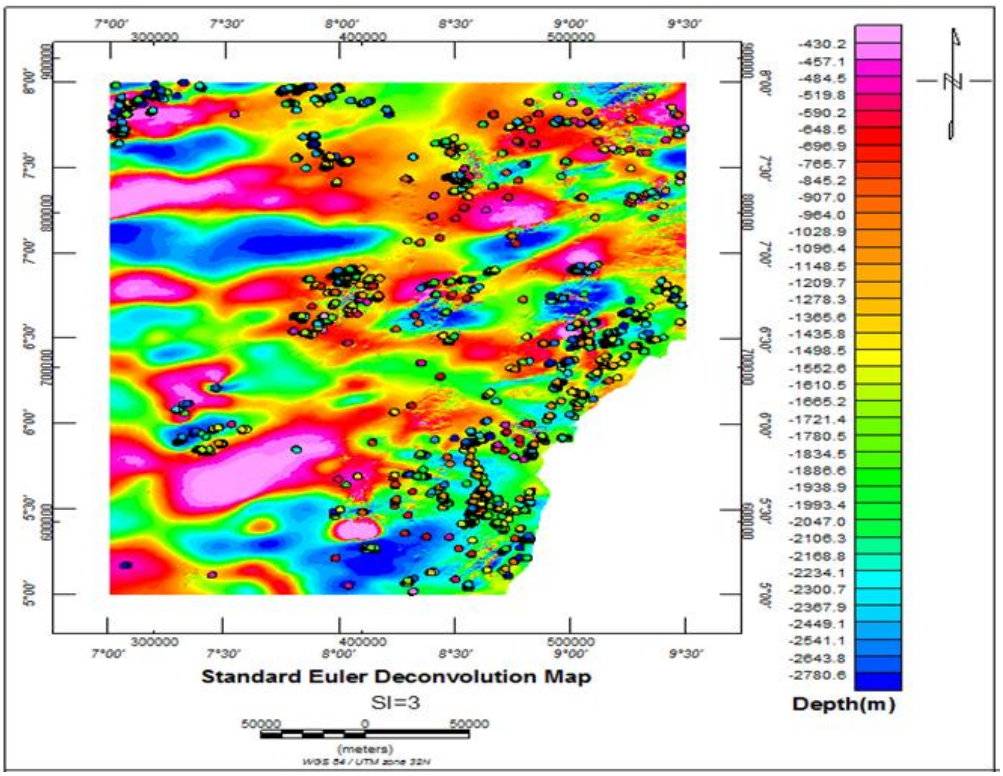

Figure 13 3D Euler deconvolution for SI = 3

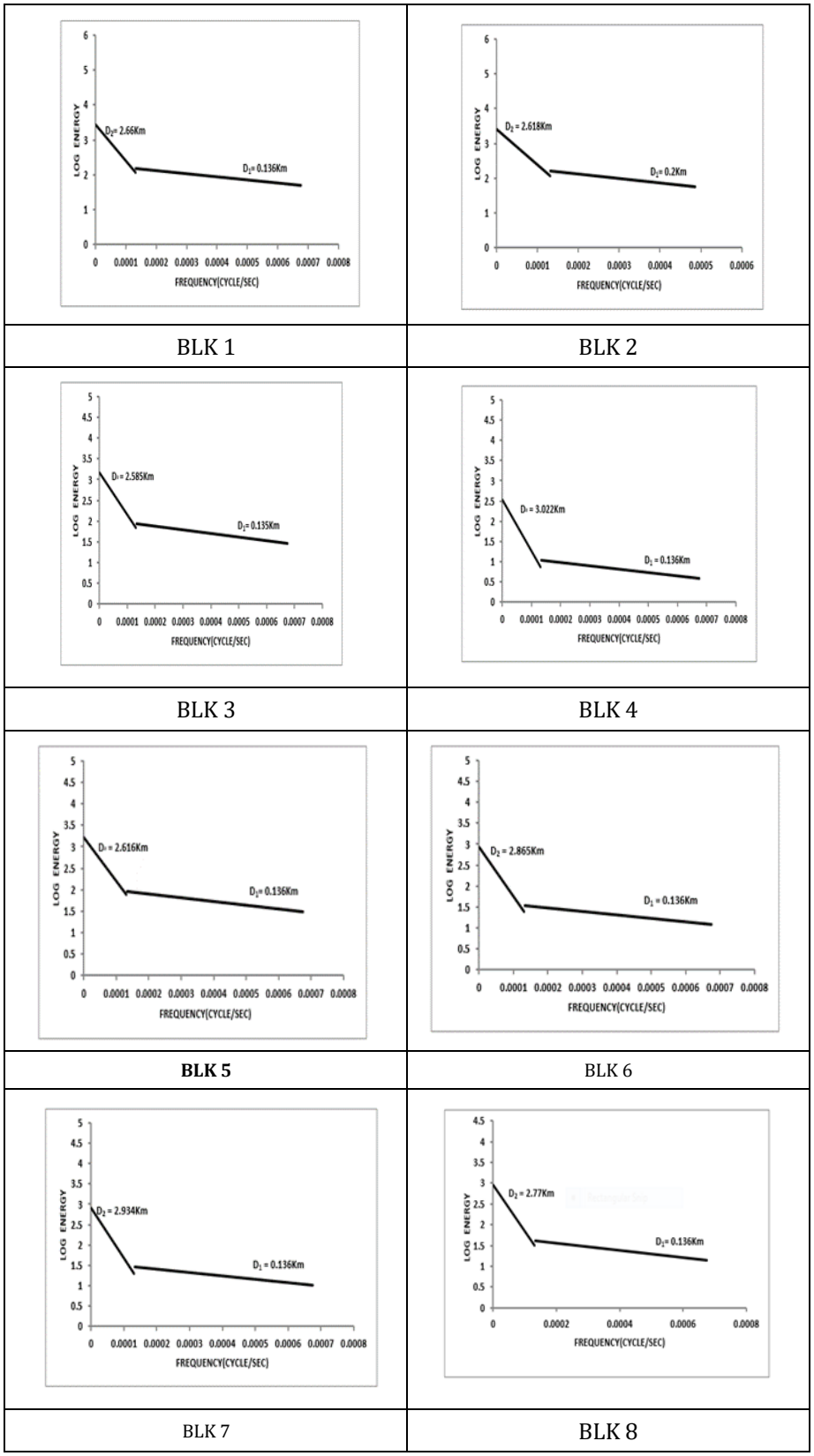

Figure 14 Sample Spectral plots of the aeromagnetic data for blocks 1 to 8

Spectral analysis was done using USGS Potential field software and Spectrum module on Matlab 7.6. To estimate the depths of the anomalies to their magnetic sources, the area was subdivided into 32 overlapping sections. Table 3 shows the computed sections. Each of these sections cover about 27.5km x 27.5km square area of the datasheet. The spectral plot is represented as spectral energies versus frequency obtained as seen in Figure 14. Each of these graphs presents

two clear segments due to deeper and shallower sources. The logarithm of the energy spectrum plot produces a straight-line graph with a resultant slope which gives a value of 2z. The average depths to magnetic causative sources were estimated from the slopes of the graphs to be D1 and D2 as shown in (Table 3). The depth (D1) is the first depth segment(layer) and it corresponds to the shallow magnetic sources while the depth (D2) is the second depth segment, which corresponds to the magnetic basement. The depth of the first layer (D1) in the study area varies between 0.135 km to 0.200 km with a mean depth of 0.158 km while the second layer (D2) varies between 2.585 km to 4.878 km with a mean depth of 3.415 km. This result, therefore, indicates that the average basement depth of the study area obtained from the spectral analysis is 3.415km. The depth to the shallow causative magnetic sources may probably be a result of tectonic activities that gave rise to basement rocks intruding into the sedimentary formation. The deeper magnetic sources may be characterized by lateral variations and basement structural deformations for example faults and fractures [15,20,27,35,46,48].

Table 2 Summary of 3D Euler depths estimation

Structural index (SI)	Depth range (m)
0	-589.3 to -2678.8
1	-459.0 to -2691.9
2	-294.6 to -2817.5
3	- 430.2 to -2780.6

Table 3 Depth to the Top of Basement (Sedimentary Thickness) of the study area

S/N	SPECTRAL BLOCKS	D1 (km)	D2 (km)
1	BLK 1	0.136	2.660
2	BLK 2	0.200	2.618
3	BLK 3	0.135	2.585
4	BLK 4	0.136	3.022
5	BLK 5	0.136	2.616
6	BLK 6	0.136	2.865
7	BLK 7	0.136	2.934
8	BLK 8	0.136	2.770
9	BLK 9	0.136	2.655
10	BLK 10	0.136	2.657
11	BLK 11	0.136	2.812
12	BLK 12	0.135	2.784
13	BLK 13	0.136	2.851
14	BLK 14	0.138	3.000
15	BLK 15	0.136	2.756
16	BLK 16	0.136	2.871
17	BLK 17	0.176	3.626
18	BLK 18	0.177	3.526
19	BLK 19	0.175	3.400
20	BLK 20	0.175	4.878

21	BLK 21	0.175	3.325
22	BLK 22	0.177	4.426
23	BLK 23	0.178	4.653
24	BLK 24	0.176	4.020
25	BLK 25	0.176	3.513
26	BLK 26	0.177	3.620
27	BLK 27	0.177	4.255
28	BLK 28	0.177	4.135
29	BLK 29	0.177	4.308
30	BLK 30	0.180	4.802
31	BLK 31	0.176	3.968
32	BLK 32	0.177	4.380
Average		0.158	3.415

5. Discussion

The study area falls within parts of the Benue Trough and is filled with Cretaceous sediments [51]. The TMI map (Figure 3) reveals magnetic intensity values ranging from -94.2 nT to 142.6 nT. However, areas with high residual magnetic intensity (Figure 5) values vary between 53.1nT to 72.8nT, while areas with low residual magnetic intensity range between -88.8nT to -35 nT. Structural trends within the study area as shown in the residual map are mainly NE-SW and NW-SE directions are in agreement with the fault orientation within the Benue Trough, with the NE-SW trends being dominant. The result from this study is in agreement with most of the depth estimation studies within the study area [1,14,23-25,30-31]. The results obtained from spectral analysis for the depth to magnetic sources vary between 2.585 km to 4.878 km for deep structures, with a mean value of 3.415km and 0.135 km to 0.200 km for the shallow structures, with a mean value of 0.158 km. For 3D Euler, depth of structural index SI = 0 varies from -589.3 m to -2678.8 m, for SI = 1 varies from -459.0 m to -2691.9 m, SI = 2 varies from -294.6 m to -2817.5 m, and SI = 3 varies from - 430.2 m to -2780.6 m. The results in the present study are in agreement with the results obtained by other researchers who had worked within the area of study. Igwesi and Umego [13] using spectral analysis estimated the depth of magnetic sources of parts of Lower Benue Trough. The result for the basement depth of the deep structures varies from 1.16 km to 6.13 km with a mean of 3.03 km while the shallow depth varies between 0.06 km and 0.37 km having an average depth of 0.22 km. This indicates that magnetic intrusive bodies are present within the sediments. Ikeh et al. [14] determined the depth to the basement of magnetic source rocks over Nkalagu and Igumale areas and calculated depth values of 2.15–5.25 km for the deep depth and 0.35–0.99 km for the shallow magnetic source bodies. Onwuemesi [28] using spectral analysis determined the sedimentary thickness of the Anambra basin to vary from 0.9km and 5.6km. Onyishi, et al. [29] obtained a maximum depth of 4409.5 and 4909.3 m from the SPI and Euler deconvolution techniques respectively showing that the sediment thickness is capable of holding hydrocarbon accumulation.

6. Conclusion

The recent high-resolution aeromagnetic data of parts of Benue Trough were employed for depth calculation of the magnetic source of the study area. The enhancement technique namely Total Magnetic Intensity Map, Reduction to pole, regional-residual separation and upward continuation maps were employed in identifying different magnetic anomalies, Structural trends representing the tectonics of the study area were observed to trend in NE-SW and N-S directions. 2-D spectral analysis and 3D Euler deconvolution methods were employed for depth determination. The result of the 2-D spectral analysis of the study area has effectively revealed a two-layer depth model. The depth of shallow magnetic sources varies from 0.135 km to 0.200 km with an average depth of 0.158 km while the depth of magnetic basement varies from 2.585 km to 4.878 km with an average depth of 3.415 km. This result, therefore, indicates that the average basement depth of the study area obtained from the spectral inversion is 3.415km. for structural index of 0 (contacts) with depths ranging from -589.3 m to -2678.8 m, for SI = 1 (sills and dykes) depth ranges from -459.0 m to -2691.9 m, for SI=2 (horizontal cylinders and pipes) depth ranges from -294.6 m to -2817.5 m, SI=3 (spheres) depth ranges from - 430.2 m to -2780.6 m. Results from 2-D spectral analysis and 3D Euler deconvolution

methods show that the study area has a sedimentary thickness that is suitable for hydrocarbon generation and accumulation.

Compliance with ethical standards

Acknowledgments

The authors are grateful to the Management of Tertiary Education Trust Fund (TETFund) Nigeria, for sponsoring this research work, for research project intervention year 2013-2014 (merged) through Federal Polytechnic Nekede Owerri, Nigeria. We also appreciate with thanks the technical and data support received from the Nigerian Geological Survey Agency (NGSA).

Disclosure of conflict of interest

There is no conflict of interest to declare by the authors.

References

[1] Ajakaiye DE. Geophysical investigations in the Benue Trough-a review. Earth Evolution Sci., 1981; 2: 110-125.

[2] Ananaba SE. Dam sites and crustal mega-lineaments in Nigeria. ITC Journal, 1991; 1: 26-29.

[3] Benkhelil J. Structure et evolution geodynamique du Basin intracontinental de la Benoue (Nigeria) Bull. Centres Rech., Explor. Prod. Elf Aquitaine. 1988; 1207: 29-128.

[4] Blakely RJ. Potential theory in gravity and magnetic applications. Cambridge University Press. 1995.

[5] Bhattacharyya BK. Continuous spectrum of the total magnetic field anomaly due to rectangular prismatic body. Geophysics, 1966; 31: 97-121.

[6] Burke K, Dessauvagie TF, Whiteman AJ. Opening of the Gulf of Guinea and the geological history of the Benue depression and Niger Delta.Nature Phys. Sci., 1971;233: 51-55.

[7] Dobrin MB, & Savit CH. Introduction to Geophysical Prospecting, McGraw Hill. 4th edition. 1988.

[8] Ekwok SE, Akpan AE, Ebong DE, Eze OE. Assessment of depth to magnetic sources using high resolution aeromagnetic data of some parts of the Lower Benue Trough and adjoining areas, Southeast Nigeria. Advances in Space Research, 2021; 67: 2104–2119.

[9] Eshanibli AS, Osagie AU, Ismail NA. Analysis of Gravity and Aeromagnetic Data to Determine Structural Trend and Basement Depth Beneath the Ajdabiya Trough in Northeastern Libya. SN Appl. Sci. 2021; 3: 228. https://doi.org/10.1007/s42452-021- 04263-7.

[10] Grant NK. South Atlantic, Benue Trough and Gulf of Guinea Cretaceous Triple Junction. Geol. Soc. Amer, Bull,1971; 82: 2295 – 2298.

[11] Gunn PJ. Application of Aeromagnetic Surveys to Sedimentary Basin Studies. AGSO Journal of Australian Geology and Geophysics, 1997;17(2): 133-144.

[12] Hahn A, Kind EG, Mishra DC. Depth estimation of magnetic sources by means of Fourier amplitude spectra. Geophysics Prospecting,1976; 24: 287-308.

[13] Igwesi ID, Umego MN. Interpretation of aeromagnetic anomalies over some parts of lower Benue Trough using spectral analysis technique. Int. J. Sci. Technol. Res., 2013; 2;153-165.

[14] Ikeh JC, Ugwu GZ, Asielue K. Spectral depth analysis for determining the depth to the basement of magnetic source rocks over Nkalagu and Igumale areas of the Lower Benue Trough, Nigeria. International Journal of Physical Sciences. 2017; 12(19): 224– 234.

[15] Kangoko R, Ojo SB, Umego MN. Estimation of Basement depths in the Middle Cross River basin by Spectral analysis of the Aeromagnetic field. Nigerian Journal of Physics, 1997; 9: 30-36.

[16] Kearey P, Brooks M, Hill J. An introduction to Geophysical exploration (Third Edition) Blackwell science Ltd. 2002.

[17] Murat RC. Stratigraphy and palaeogeography of the Cretaceous and Lower Tertiary in Southern Nigeria. In African Geology. ed. T. J. F. Dessauvigie and A. J.Whiteman, University of Ibadan Press.1972; 635 – 648.

[18] Murphy BS. Airborne geophysics and the Indian scenario. Indian Geophysics Union Journal, 2007;11(1): 1-28.

[19] Nwachukwu SO. Approximate geothermal gradients in Niger Delta sedimentary basin. American Association of Petroleum Geologists Bulletin, 1972; 60(7): 1073 – 1077.

[20] Nwokocha KC, Opara AI, Onyekuru SO, Okereke CN, Emberga TT, Ugwugbu EI, Ijeoma KC. Lineament features interpreted over parts of Younger Granite Complex, North Central Nigeria using HRAM and LANDSAT-ETM data. Arabian Journal of Earth Science (AJES), 2016; 3(1): 35-56.

[21] Obaje NG. Origin of the Benue Trough- A critical Review. In: Geology of Nigeria. C.A. Kogbe, (ed). Elizabeth Publishing Co., Lagos, Nigeria. 2004.

[22] Obaje NG. Geology and mineral resources of Nigeria. Berlin: Springer Publishers. 2009; 1–203.

[23] Obiora DN, Oha IA, Ihedike OA, Igwe E. Comparative depth estimates and modelling of magnetic anomalies over the Nkalagu area, Southeastern Nigeria. Modeling Earth Systems and Environment. 2021; 8:1291–1309.

[24] Ofoegbu CO, Onuoha MK. Analysis of magnetic data over the Abakaliki Anticlnirium of the Lower Benue Trough, Nigeria. Marine and Petroleum Geology, 1991; 8(2): 174 – 183.

[25] Oha IA, Onuoha KM, Nwegbu AN, Abba AU. Interpretation of high resolution aeromagnetic data over southern Benue Trough, Southeastern Nigeria. J. Earth Syst. Sci. 2016;125: 369–385.

[26] Olade MA. Evolution of Nigeria's Benue Trough (aulacogen): A tectonic model. Geol. Mag.1975; 112: 576-583.

[27] Ole MO, Opara AI, Okereke CN, Onyenegecha CP, Akaolisa CZ, Okoli AE, Umoh OJ. Estimates of the Curie Point Depth, Geothermal Gradient and Near Surface Heat Flow System of Bida and Environs, Nupe Basin Nigeria from High-Resolution Aeromagnetic Data. International Journal of Energy and Water Resources, 2020; 108 (Springer).DOI: 10.1007/s42108-020-00108-y.

[28] Onwuemesi AG. One-Dimensional Spectral Analysis of Aeromagnetic Anomalies and Curie Depth Isotherm in the Anambra Basin of Nigeria. J. Geodynamics, 1997; 23(2); 95-107.

[29] Onyishi GE, Ugwu GZ. Source Parameter Imaging and Euler Deconvolution of Aeromagnetic Anomalies over Parts of the Middle Benue Trough, Nigeria. American Journal of Geophysics, Geochemistry and Geosystems.2019; 5(1): 1-9.

[30] Onyewuchi RA, Opara AI, Ahiarakwem CA, Oko FU. Geological interpretations inferred from airborne magnetic and Landsat data: A case study of Nkalagu area, southeastern Nigeria. Int J Sci Technol. 2012; 2: 178–191.

[31] Opara AI. Estimation of the Depth to Magnetic Basement in Part of the Dahomey Basin, Southwestern Nigeria. Australian Journal of Basic and Applied Sciences, 2011; 5(9): 335-343.

[32] Opara AI, Ekwe AC, Okereke CN, Oha IA, Nosiri OP. Integrating Airborne Magnetic and Landsat Data for Geologic Interpretation over part of the Benin Basin,Nigeria. Pacific Journal of Science and Technology, 2012; 13(1): 556-571.

[33] Opara AI, Onyewuchi RA, Selemo AO, Onyekuru SO, Ubechu BO, Emberga TT, Ibim DF, Nosiri OP. Structural and Tectonic Features of Ugep and Environs, Calabar Flank, Southeastern Nigeria: Evidences from aeromagnetic and Landsat-ETM data. Mitteilungen Klosterneuburg, 2014a; 64: 33-54.

[34] Opara AI, Oneyekuru SO, Mbagwu EC, Emberga TT, Ijeomah KC, Nwokocha KC. Integrating Landsat – ETM and Aeromagnetic Data for Enhanced Structural Interpretation over Naraguta Area, North-Central Nigeria. International J. of Scientific and Engineering Research, 2015; 6(9): 10.

[35] Opara AI, Nwofor VU, Echetama HN, Emberga TT, Inyang GE. Magnetic Basement Depth and Structure over parts of Bida Basin Nigeria interpreted from 2-D Spectral Analysis and Euler Deconvolution; Australian Journal of Basic and Applied Sciences, 2018a;12(9): 1-11.DOI.10.22587/ajbas.2018.12.9.1.

[36] Opara AI, Odumosu GE, Akaolisa CZ, Onyekuru SO, Emberga TT, Onu NN. Basement Depth Re-Evaluation and Structural Kinematic Analysis of Part of the Middle Benue Trough using High-Resolution Aeromagnetic Data. Futo Journal Series. 2018b; 4(1); 409 – 436.

[37] Reid B, Allsop JM, Granser H, Millet AJ, Somerton IW. Magnetic interpretation in three dimensions using Euler deconvolution, Geophysics, 1990; 55(1): 80-91.

[38] Reid AB, Ebbing J, Webb SJ. Avoidable Euler errors— the use and abuse of Euler deconvolution applied to potential fields. Geophysics Prospect. 2013;

[39] Reyment RA. Aspects of the geology of Nigeria: The stratigraphy of the Cretaceous and Cenozoic deposits. University of Ibadan Press. 1965; 133.

[40] Reynolds JM. An introduction to Applied and Environmental Geophysics. 1st edition. John Wiley and Sons. 1997.

[41] Salawu NB. Dada SS, Fatoba JO, Ojo OJ, Adebiyi LS, Sund AJ, Abdulraheem TY. Structural architecture of the Middle Niger Basin, Nigeria based on aeromagnetic data: An example of a non-volcanic basin. 2021;7: 1-9.

[42] Short KC, Stauble AJ, Outline the geology of the Niger Delta. American Assoc. Petrol. Geol. Bull.1967; 51: 761-779.

[43] Telford WM, Geldart LP, Sheriff RE. Applied Geophysics. 2nd Edition. Cambridge University Press. 1990.

[44] Ugwu CM, Ugwu GZ. Euler deconvolution and forward and inverse modelling of aeromagnetic anomalies over Ogoja and Bansara areas of Lower Benue Trough, Nigeria. Amer. J. Geophys. Geochem. Geosyst., 2018; 4(1): 1-12.

[45] Whiteman AJ. Nigeria: Its petroleum geology resources and potential.Graham and Trotham, London, 1982; 2: 306–361.

[46] Emberga TT, Opara AI, Echetama HN, Udoka OP, Inyang GA.' Magnetic Basement Depth Re-evaluation over the Yola Arm of the Upper Benue Trough, Nigeria from 3-D Euler Deconvolution and Spectral inversion of HRAM data. International Journal of Scientific & Engineering Research,2016; 7(4); 538-551.

[47] Onyewuchi RA, Ugwu SA. Geological Interpretation of the High Resolution Aeromagnetic Data over Okigwe-Udi Area, Anambra Basin, Nigeria, Using 3-D Euler Deconvolution and 2-D Spectral Inversion Methods. Journal of Geography, Environment and Earth Science International. 2015; 10(1); 1-22.

[48] Opara AI, Onyewuchi RA, Okonkwo AC, Nosiri OP, Emberga TT. Structural interpretation of the Afikpo sub-basin: evidence from airborne magnetic and Landsat ETM data; Elixir Earth Sci. 2014b; 71: 24546-24552.

[49] Udensi EE, Osazuwa IB. Spectral determination of depth to buried magnetic rocks under the Nupe Basin, Nigeria. Nigerian Association of Petroleum Explorationists Bulletin, 2004; 17(1): 22-27.

[50] Umeanoh DC, Ofoha CC, Ugwu SA. Spectral Analysis and Euler Deconvolution of Regional Aeromagnetic Data to Delineate Sedimentary Thickness in Mmaku Area, South Eastern Nigeria. World Scientific News, 2018;109: 26-42.

[51] Ofoegbu CO. Interpretation of aeromagnetic anomalies over Lower and Middle Benue Trough of Nigeria. Geophys. J. Royal Astronom. Soc. 1984; 79: 813–823.

[52] Spector A, Grant FS. Statistical models for interpreting aeromagnetic data. Geophysics, 1970; 35: 293-302.

[53] Thompson DT. 1982. EULDPH: A new technique for making computer-assisted depth estimates from magnetic data. Geophysics, 1982; 47 (1): 31-37.